

# SharedAssembly: A Data Collection Approach via Shared Tele-Assembly

Yansong Wu<sup>†,1</sup>, Xiao Chen<sup>†,1</sup>, Yu Chen<sup>1</sup>, Hamid Sadeghian<sup>1</sup>, Fan Wu<sup>1</sup>, Zhenshan Bing<sup>1</sup>,  
Sami Haddadin<sup>2</sup>, Alexander König<sup>1</sup>, Alois Knoll<sup>1</sup>

**Abstract**—Assembly is a fundamental skill for robots in both modern manufacturing and service robotics. Existing datasets aim to address the data bottleneck in training general-purpose robot models, falling short of capturing contact-rich assembly tasks. To bridge this gap, we introduce *SharedAssembly*, a novel bilateral teleoperation approach with shared autonomy for scalable assembly execution and data collection. User studies demonstrate that the proposed approach enhances both success rates and efficiency, achieving a 97.0% success rate across various sub-millimeter-level assembly tasks. Notably, novice and intermediate users achieve performance comparable to experts using baseline teleoperation methods, significantly enhancing large-scale data collection.

## I. INTRODUCTION

The general-purpose intelligent robot has long been regarded as the “ultimate goal” of the robotics community, pursued by scientists for decades. In recent years, the groundbreaking success of foundation models in language and vision [1], [2] has reignited enthusiasm in the field. Researchers are increasingly integrating these models into robotics, fostering rapid advancements and innovation [3]. Compared to traditional robot learning models trained on limited datasets, this paradigm shift underscores the growing importance of large-scale, diverse, and high-quality datasets, which are crucial for achieving robust and general-purpose performance.

Some researchers have actively developed low-cost data collection devices to lower the entry barrier to data acquisition [4]–[7], facilitating the generation of more diverse and comprehensive datasets. Concurrently, an increasing number of large-scale open-source datasets have been created over recent years for training foundation robotic models, as shown in Table I. These efforts seek to mitigate the data bottleneck in model training. However, most existing works primarily focus on expanding the number of simple tasks and scenes without considering the diversity of tasks. Consequently, a significant portion of these datasets consists of relatively simple manipulation tasks, such as picking, placing, pushing, and object rearrangement. Contact-rich manipulation challenges, such as assembly, remain underexplored. This dataset imbalance significantly limits the upper bound of model performance on complex contact-rich manipulation tasks. As the predominant method for real-world robotic manipulation data acquisition, human teleoperation inherently

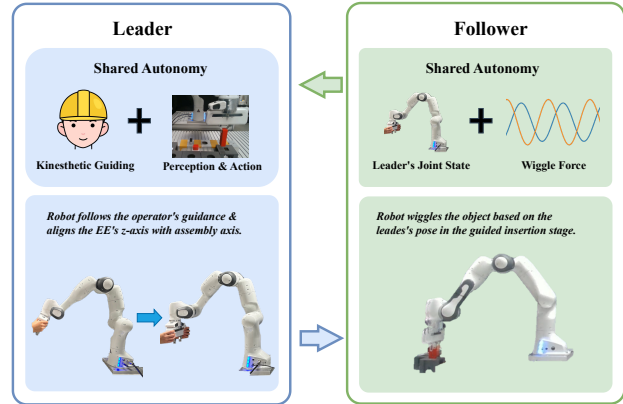


Fig. 1: Illustration of the proposed approach for data collection in contact-rich assembly by shared tele-assembly.

struggles with handling contact-rich tasks due to the lack of transparency and complex high dimension in task space (a detailed analysis is provided in Sec. II-B).

To address this problem, we propose *SharedAssembly*, a novel bilateral teleoperation approach with shared autonomy for executing assembly and data collection tasks. It incorporates the knowledge for solving tight-clearance assembly tasks [8]–[11] into robot teleoperation through shared autonomy. By delegating part of the autonomy to the leader and follower, *SharedAssembly* reduces the complexity of human operation in contact-rich tele-assembly, significantly improving success rates and execution efficiency. Consequently, it paves the way for large-scale data acquisition for contact-rich manipulation tasks through teleoperation.

The main contributions of this paper are:

- A bilateral teleoperation framework with shared autonomy for data collection in contact-rich manipulation tasks at scale.
- Incorporating force domain actions for solving tight-clearance assembly tasks to enhance teleoperation performance and efficiency.
- A user study for the effects of teleoperation methods across operators with varying experience levels, demonstrating the strong potential in large-scale data acquisition.

## II. RELATED WORKS

In this section, we focus our review on (i) Robot Manipulation Dataset, (ii) Teleoperation System for Data Collection and (iii) Shared Teleoperation.

<sup>†</sup> The authors contribute equally.

<sup>1</sup> The authors are with the Chair of Robotics and Systems Intelligence, MIRMI - Munich Institute of Robotics and Machine Intelligence, Technical University of Munich, Germany.

<sup>2</sup> The author is with Mohamed bin Zayed University of Artificial Intelligence, Abu Dhabi, UAE

Dataset	# Traj.	# Skills	# Average Traj. / Skill	# Assembly Traj.	Collection Method
RT1 [12]	130k	8	16.2k	none	Human Teleoperation
MIME [13]	8.3k	20	0.4k	none	Kinesthetic Teaching
BC-Z [14]	26k	3	8.6k	none	Human Teleoperation
RH20T [15]	110k	42	2.6k	1.6k	Human Teleoperation
RoboSet [16]	98.5k	12	8.2k	none	30% Human / 70% Scripted
BridgeData V2 [17]	60.1k	13	4.6k	none	85% Human / 15% Scripted
DROID [18]	76k	86	0.8k	1	Human Teleoperation
Open X-Embodiment [19] <sup>†</sup>	1.4M	217	64.8k	9.8k	Dataset Aggregation

TABLE I: Summary of existing real-world datasets for training robot model. The notation “#” refers to the number. <sup>†</sup>only the aggregation of existing datasets instead of an independent novel dataset.

### A. Robot Manipulation Dataset

Real-world data plays a vital role in training robotic models. Traditional datasets often lack diversity, typically focusing on a single task, a limited set of objects, or a narrow range of environments. As general-purpose pre-trained models have achieved significant success in natural language processing (NLP) and computer vision, there is an increasing emphasis on dataset diversity in robotic manipulation [12]–[20].

In robotics, the complexity of manipulation tasks varies significantly. This variation also affects data acquisition, leading to a substantial imbalance in task distribution within datasets. As summarized in Table I, the number of trajectories for contact-rich manipulation tasks, such as assembly, is significantly lower than the dataset average. A recent study addresses this issue by creating a human teleoperation-based dataset specifically designed for assembly tasks [21]. However, due to the inherent difficulty of these tasks, collecting such a dataset requires extensive human effort. Consequently, more than 10% of the data consists of failed trials.

### B. Teleoperation System for Data Collection

As shown in Table I, human teleoperation has emerged as the predominant method for acquiring real-world robotic datasets at scale. Based on the direction of the signal flow, the teleoperation system can be categorized into two types: 1) **Unilateral Teleoperation** in which the signal is transmitted solely from the leader to the follower, and 2) **Bilateral Teleoperation**, which includes a feedback loop from the follower to the leader, enabling the operator to perceive the remote environment.

The majority of the teleoperation systems utilized in data collection employ input devices such as space mouse or virtual reality (VR) remotes [12], [14], [16]–[18]. However, these devices do not provide force feedback, which complicates the execution of contact-rich tasks and increases the risk of unsafe interactions. Furthermore, due to workspace mismatches, the follower robot is prone to encountering singularities. To mitigate these issues, some studies have proposed input devices designed based on the kinematics of the follower robot [6], [7], [22] which also lack force feedback. Bilateral teleoperation, by incorporating force feedback, enhances user interaction with the remote environment, thereby improving task performance and increasing demonstration success rates [23]. Recognizing the importance of force feed-

back, a recent research has incorporated it into teleoperation devices [24].

Haptic devices are commonly employed in teleoperation systems when force feedback is required [15], [21], facilitating data collection for assembly tasks. However, due to morphological differences between haptic devices and execution robots, as well as the unrealistic interaction forces they generate, demonstrations using these devices often lack intuitiveness [25]. To address these limitations, this study adopts a teleoperation system consisting of two identical robot arms, following the approach in [26], to ensure maximum intuitiveness and transparency.

### C. Shared Teleoperation

The direct teleoperation of multi-DoF tasks is challenging, even in a system with high transparency. It often requires extensive training and demands significant mental acuity and proficiency. To address this, shared autonomy leverages the prior knowledge to assist human operators from different perspectives [27]. This approach has been applied to the teleoperation system to improve safety [28] and increase intuitiveness [29]. In [30] a shared control template is proposed where some task space coordinates are fixed or constrained to assist the users in task execution. Additionally, shared autonomy can mitigate the influence of time delays and improve the task performance [31], leading to stability and ensuring that the delayed visual feedback does not degrade the performance. Furthermore, supervised autonomy has been applied in [14] where the users monitor the robot’s execution and intervene when the robot tends to fail.

## III. PRELIMINARIES: BILATERAL TELEOPERATION

In this section, the basic position-force bilateral teleoperation architecture is first presented. The proposed shared tele-assembly is then introduced in the next section.

A basic Position-Force (P-F) architecture for a bilateral teleoperation system is illustrated in Fig. 2. The joint velocity of the leader robot is transmitted through the communication channel to the follower robot as its desired velocity to track. In the other direction, the interaction force between the follower robot and the environment is transmitted back to the leader robot and applied to the operator’s hand to feel the remote environment.

Consider a torque-controlled robot with  $n$ -DoF, and ignoring the joint friction, the dynamics of a robot manipulator in

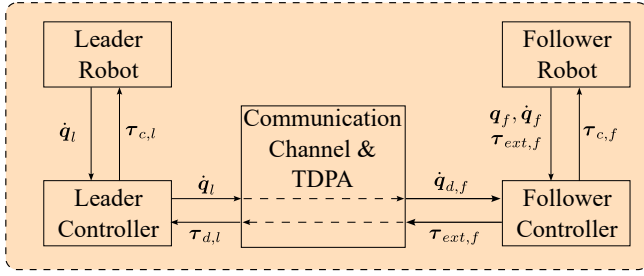


Fig. 2: Structure of basic bilateral teleoperation.

joint space is written as:

$$\mathbf{M}_i(\mathbf{q}_i)\ddot{\mathbf{q}}_i + \mathbf{c}_i(\mathbf{q}_i, \dot{\mathbf{q}}_i) + \mathbf{g}_i(\mathbf{q}_i) = \boldsymbol{\tau}_{c,i} + \boldsymbol{\tau}_{ext,i} \quad (1)$$

where  $\mathbf{M}_i \in \mathbb{R}^{n \times n}$  corresponds to the mass matrix,  $\mathbf{c}_i \in \mathbb{R}^n$  indicates the Coriolis/centrifugal vector. The vectors  $\mathbf{q}_i, \dot{\mathbf{q}}_i, \ddot{\mathbf{q}}_i \in \mathbb{R}^n$  represent the robot joint position, velocity, and acceleration. The parameter  $\boldsymbol{\tau}_{c,i} \in \mathbb{R}^n$  is the command torque to the robot and  $\boldsymbol{\tau}_{ext,i} \in \mathbb{R}^n$  is the external torque applied on the robot. The subscript  $i \in \{l, f\}$  represents *leader* and *follower*, respectively.

1) *Leader*: As the leader robot serves as an intuitive input device, it is expected to provide the operator with a lightweight and responsive interface while simultaneously conveying force feedback from the follower. The control on the leader side is mainly a gravity compensation controller given by,

$$\boldsymbol{\tau}_{c,l} = \mathbf{g}_l(\mathbf{q}_l) + \mathbf{c}_l(\mathbf{q}_l, \dot{\mathbf{q}}_l) + \boldsymbol{\tau}_{d,f}, \quad (2)$$

where  $\boldsymbol{\tau}_{d,f}$  denotes the torque generated by external forces on the follower's joints transmitted back to the leader.

2) *Follower*: The follower robot is designed to synchronize with the leader's movements. A joint impedance control strategy is employed to track the leader's position and velocity, as follows:

$$\boldsymbol{\tau}_{c,f} = \mathbf{K}_q \mathbf{e}_q + \mathbf{D}_q \dot{\mathbf{e}}_q + \mathbf{c}_f(\mathbf{q}_f, \dot{\mathbf{q}}_f) + \mathbf{g}_f(\mathbf{q}_f), \quad (3)$$

where the joint error and velocity error are expressed as  $\mathbf{e}_q = \mathbf{q}_{d,f} - \mathbf{q}_f$ , and  $\dot{\mathbf{e}}_q = \dot{\mathbf{q}}_{d,f} - \dot{\mathbf{q}}_f$ , respectively. The parameters  $\mathbf{K}_q \in \mathbb{R}^{n \times n}$  and  $\mathbf{D}_q \in \mathbb{R}^{n \times n}$  represent the positive definite stiffness and damping matrices for the tracking controller. Moreover,  $\mathbf{q}_{d,f}, \dot{\mathbf{q}}_{d,f}$  are the position and velocity of the leader that are received on the follower side as desired values.

In order to preserve passivity and thus stability of teleoperation, the Time Domain Passivity Approach (TDPA), adapted from [32], is implemented in this study. The effect of time delay falls outside the scope of this work and is not considered.

#### IV. PROPOSED SHARED TELE-ASSEMBLY

As illustrated in Fig. 1, the human operator kinaesthetically guides the leader which acts as an input device to control the follower, conveying human intention and enabling the follower to interact with the real-world environment. From the perspective of command flow, the system can be conceptualized as a hierarchical structure with three layers [33]. In a well-organized system, members collaborate

simultaneously to achieve a common goal. Each layer is responsible for tasks at different granularity levels [34].

In the context of assembly and specifically for peg in hole tasks, after picking up the part, the process consists of two stages: (i) *Position Guiding*: The operator manipulates the leader's End-Effector (EE) to reach the target assembly area. (ii) *Guided Insertion*: The robot aligns the assembly object with the assembly axis and completes the insertion, requiring precise control of both the follower EE's position and orientation.

However, in real teleoperation scenarios, camera perspective distortion makes it difficult for the operator to accurately perceive spatial information. Besides, the operator must adapt the mismatch between the camera view and her/his natural field of view. Consequently, achieving accurate control over the object's pose — particularly its orientation — becomes significantly more challenging.

To address this issue, we decompose the problem into subtasks of different granularity and redistribute part of the original operator's workload to the leader and follower using a shared autonomy strategy. As a result, the human operator, leader and follower share the autonomy in a following manner:

- The **human operator** focuses primarily on coarse-grained task, *i.e.*, controlling the object's trajectory to accomplish the overall task.
- The **leader** takes responsibility for medium-grained task, assisting the operator in maintaining a roughly aligned orientation throughout the whole assembly process.
- The **follower** handles the fine-grained task, namely fine-tuning the object's orientation during the guided insertion stage.

Building on this autonomy sharing strategy, the original bilateral teleoperation framework is enhanced as follows:

1) *Shared autonomy on leader side*: To preserve the user's dominance, the leader merely assists the operator in maintaining the EE's spatial orientation along the  $z$ -axis rather than fully locking its orientation. Consequently, the operator retains control over the robot's position and rotation along the insertion axis, which is crucial for assembly tasks involving non-cylindrical objects.

Therefore, the operator can still manipulate the robot's position and the rotation along the  $z$ -axis, which is crucial for assembly tasks involving non-cylindrical objects.

To align EE's  $z$ -axis  $\mathbf{z}_l$  with the target direction  $\mathbf{z}_{target}$ <sup>1</sup> with minimal intervention, the leader's desired goal orientation is determined by rotating the current EE frame's orientation by an angle  $\theta$  along the axis  $\mathbf{a}_r$ , as defined by the following equations:

$$\begin{aligned} \mathbf{a}_r &= \mathbf{z}_l \times \mathbf{z}_{target}, \\ \theta &= \arccos(\mathbf{z}_l \cdot \mathbf{z}_{target}). \end{aligned} \quad (4)$$

Then, the above error in angle/axis representation is then converted to Euler angle for calculating the desired goal pose

<sup>1</sup>In this paper, the unit vector  $\mathbf{z}_{target}$  is obtained by estimating the surface normal of the assembly hole using the PCL library.

Task	Peg Shape	Peg Geometry (mm)	Peg		Hole		Clearance (mm)
			Material	Manufacturing	Material	Manufacturing	
A	Cylinder	length: 50, diameter: 40	PAM	CNC	PLA	3D printing	0.25
B	Cylinder	length: 50, diameter: 40	PAM	CNC	PLA	3D printing	0.13
C	Cylinder	length: 50, diameter: 40	PAM	CNC	PLA	3D printing	0.07
D	Cuboid	length: 35, width: 25, height: 60	PLA	3D printing	PLA	3D printing	0.10
E	Hexagonal Prism	length: 50, side length: 11	PLA	3D printing	PLA	3D printing	0.10
F	Cylinder	length: 50, diameter: 20	PAM	CNC	Aluminum	CNC	0.02

TABLE II: Task objects configuration. Tasks A, B, and C share the same peg, differing only in hole size.

$p_d$ . The original leader's control law is enhanced as:

$$\begin{aligned} \tau_{c,l} = & \mathbf{J}_l^T(\mathbf{q}_l) \mathbf{A}_1 [\mathbf{K}_c(\mathbf{p}_d - \mathbf{p}_l) - \mathbf{D}_c \dot{\mathbf{p}}_l] \\ & + \mathbf{c}_l(\mathbf{q}_l, \dot{\mathbf{q}}_l) + \mathbf{g}(\mathbf{q}_l) + \tau_{d,f}, \end{aligned} \quad (5)$$

where  $\mathbf{J}$  is the Jacobian matrix, and  $\mathbf{A}_1 = \text{diag}(0, 0, 0, 1, 1, 0)$  is a selection matrix. Moreover matrices  $\mathbf{K}_c \in \mathbb{R}^{6 \times 6}$  and  $\mathbf{D}_c \in \mathbb{R}^{6 \times 6}$  represent the Cartesian stiffness and damping matrices. The leader's current pose and velocity are expressed as  $\mathbf{p}_l$  and  $\dot{\mathbf{p}}_l$ , respectively.

2) *Shared autonomy on follower side*: In contrast to the leader, which assists the operator throughout the entire assembly process, the follower only shares autonomy during the guided insertion stage by fine-tuning the object's orientation. Due to the limitations in perception accuracy in estimating the target direction  $\mathbf{z}_{target}$ , naively following the leader's motion often results in task failure, particularly in tight-clearance assembly tasks. To address this issue, we incorporate force domain knowledge on tight-clearance robotic assembly into the system's assistance, *i.e.*, leveraging a feedforward force  $\mathbf{f}_{ff}$  based wiggle motion to mitigate this error [9], [10]. This wiggle motion is regulated by the autonomy level  $\eta$ , which is determined by the operator's intention and execution situation.

$$\eta = \begin{cases} 1, & \|\mathbf{f}_{ext,f,xy}\| > f_t, \\ 0, & \text{else,} \end{cases} \quad (6)$$

where  $\mathbf{f}_{ext,f,xy}$  represents the external force applied on the EE in  $xy$  plane indicating the constraint force during insertion. Moreover,  $f_t$  is a detection threshold. The feedforward term is designed as:

$$f_{ff,j}(t) = a_j \cdot \sin(2\pi f_j t + \varphi_j), \quad (7)$$

where  $a_j$ ,  $f_j$  and  $\varphi_j$  refer to the amplitude, frequency and phase, respectively. The subscript  $j$  refers to the direction in the range  $\{x_f, y_f, z_f, rx_f, ry_f, rz_f\}$  of the EE frame, and  $t$  indicates the execution time.

According to our autonomy-sharing mechanism, the robot assumes control over the Cartesian pose's  $rx$  and  $ry$  components, preventing the user from experiencing external forces along the corresponding axes. Thus, a selection matrix  $\mathbf{A}_2 = \text{diag}(0, 0, 0, 1, 1, 0)$  is chosen to apply the force domain knowledge on the corresponding dimension. Consequently, the follower's control law is updated as follows:

$$\begin{aligned} \tau_{c,f} = & \mathbf{K}_q \mathbf{e}_q + \mathbf{D}_q \dot{\mathbf{e}}_q + \mathbf{c}_f(\mathbf{q}_f, \dot{\mathbf{q}}_f) + \mathbf{g}_f(\mathbf{q}_f) \\ & + \eta \mathbf{J}^T(\mathbf{q}_f) \mathbf{A}_2 \mathbf{f}_{ff}. \end{aligned} \quad (8)$$

To increase the legibility and predictability of the system, and reduce the disturbance applied to the operator, the moment part of the external force is not transmitted back to the operator. Therefore, the feedback torque transmitted to the leader  $\tau'_{ext,f}$  is:

$$\tau'_{ext,f} = \mathbf{J}_f^T(\mathbf{q}_f) \mathbf{A}_3 \mathbf{f}_{ext,f}, \quad (9)$$

where  $\mathbf{A}_3 = \text{diag}(1, 1, 1, 0, 0, 0)$  refers to the selection matrix for regulating the force feedback, and  $\mathbf{f}_{ext,f} \in \mathbb{R}^6$  indicates the external force applied on the follower's EE.

## V. EXPERIMENTAL STUDY

### A. Data Collection Setup

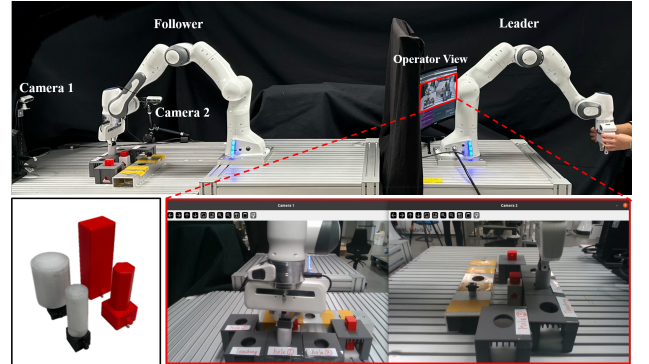


Fig. 3: Experimental setup for data collection based on shared tele-assembly

As illustrated in Fig. 3, the experimental setup comprises three platforms (arranged from left to right) to accommodate the insertion tasks, the follower robot, and the leader robot, respectively. The detailed configuration of each insertion object is provided in Table II. Both manipulators are Franka Emika Panda robots. The leader robot is controlled by a PC running Ubuntu 20.04 with Intel Core i7-10700 CPU, while the follower is controlled by another PC running Ubuntu 20.04 with Intel Core i9-11900K CPU. Two PCs communicate through User Datagram Protocol (UDP) within the same network, making network delay negligible. Additionally, two Intel RealSense D435i cameras are mounted on the follower's side, positioned vertically to provide stereo views for the human operator.

### B. Experimental Design

As detailed in Sec. II-B, the teleoperation approaches in data collection can be broadly categorized based on

Parameter	Value
$K_c$	diag(0, 0, 0, 35, 35, 0)
$K_q$	diag(450, 450, 450, 300, 150, 75, 45)
$[a_{rx}, a_{ry}]$	[0.766, 0.906]
$[f_{rx}, f_{ry}]$	[2.150, 2.160]
$[\varphi_{rx}, \varphi_{ry}]$	[-1.562, 0.610]

TABLE III: Control parameters utilized in the experiment.

whether the operator receives contact force feedback from the follower robot. To validate the effectiveness of our proposed method **SharedAssembly**, we conducted a user study and selected one representative baseline method from each category for comparison, *i.e.*, **Unilateral Teleoperation** in which force feedback is not employed on leader robot, and **Bilateral Teleoperation** which enables the operator to perceive interaction forces occurring at the leader side [31].

Building upon these, we designed our user study to compare the performance across six tight-clearance assembly tasks detailed in Table II. To ensure reliable results, 29 participants were invited. Based on their prior experience with teleoperation and robot, they were categorized into three groups:

- **Expert** ( $n = 8$ ): Participants with teleoperation experience.
- **Intermediate** ( $n = 10$ ): Participants with prior experience in robotics but not teleoperation.
- **Novice** ( $n = 11$ ): Participants with no prior experience in robotics.

The user study procedure consists of three phases: In phase I, the participants complete 3 training trials using a training hole with large clearance to familiarize themselves with the teleoperation system and the task. In phase II, task A, B, and C are conducted as a large batch of trials to assess the influence of clearance on task performance. In the phase III, task D, E, and F are conducted separately to examine the impact of different peg shapes. For each task, each participant repeated three times across all three experimental conditions. To minimize the effects of *sensorimotor adaptation* in human skill acquisition [35], the teleoperation method and task are randomly assigned in each trial. In addition, the participants were blinded to the teleoperation method they were using, to mitigate the influence of cognitive expectations on performance. The concrete controller’s parameters are detailed in Table III. Each trial is restricted to a maximum duration of 60s, with 30s allocated to each task stage. Trials that exceed the time limit or violate the robot’s safety margin are considered failures and recorded as 60s.

Method	A	B	C	D	E	F	Average
Unilateral	96.3	75.3	48.2	63.2	73.3	48.1	67.4
Bilateral	<b>100.0</b>	95.3	66.7	94.7	<b>95.1</b>	90.4	91.0
SharedAssembly	<b>100.0</b>	<b>100.0</b>	<b>94.1</b>	<b>100.0</b>	93.9	<b>94.1</b>	<b>97.0</b>

TABLE IV: Success Rate [%]

## VI. RESULT & DISCUSSION

To obtain a more accurate experimental result, we use the object’s front-end reaching the hole area as a trigger

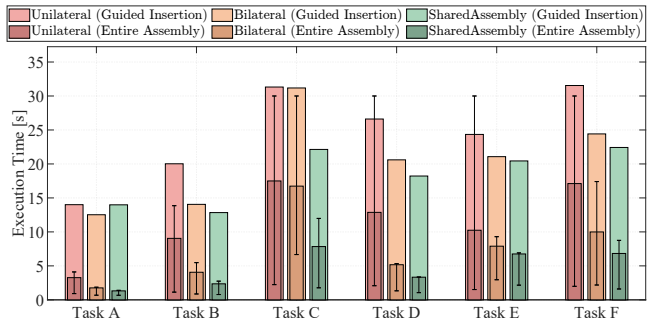


Fig. 4: Task execution time. The darker-color columns with interquartile range indicators represent the execution time during the guided insertion phase; The lighter-color columns correspond to the total execution time, encompassing both the position guiding phase and the guided insertion phase.

event, dividing the entire assembly process into the two stages detailed in Sec. IV. The concrete execution time of each stage is illustrated respectively in Fig. 4. During the position-guiding phase, the performance of all methods is comparable, with no evidence indicating superiority. In contrast, in the guided insertion phase, a clear performance hierarchy emerges, with *SharedAssembly* demonstrating the best performance, followed by *Bilateral* teleoperation, and *Unilateral* teleoperation performing the worst. Meanwhile, our approach exhibits the highest robustness, as indicated by the narrowest interquartile range.

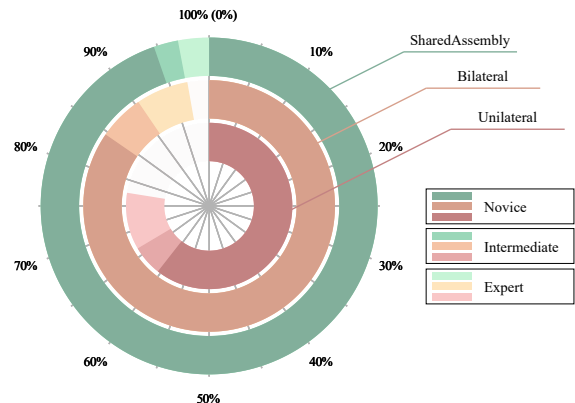


Fig. 5: Overall success rate for all tasks across participants with different backgrounds.

The entire task completion time (Fig. 4) and the overall task success rate (TABLE IV) follow the same trend. Considering that tasks A, B, and C only differ in the hole diameter, the corresponding result distinctly demonstrates the effect of the task’s clearance on the approach’s performance. As task clearance decreases, the success rates of *Unilateral* and *Bilateral* Teleoperation drop by around 50% and 33%, respectively. In contrast, our approach’s success remains a 94.1% success rate, showcasing remarkable ability in handling tight-clearance assembly tasks.

Fig. 5 illustrates the overall success rate of participants with varying levels of background knowledge. Compared to those without teleoperation experience, experienced partic-

## ACKNOWLEDGMENT

We sincerely thank the 29 volunteers for their participation in our experiment and their valuable contributions to our data collection. Besides, we acknowledge the financial support by the Federal Ministry of Education and Research of Germany (BMBF) in the program of “Souverän. Digital. Vernetzt.” Joint project 6G-life, project identification number 16KISK002. We gratefully acknowledge the funding of the Lighthouse Initiative Geriatrics by LongLeif GaPa gGmbH (Project Y) and the funding of the Lighthouse Initiative KIFABRIK Bayern by StMWi Bayern, Forschungs- und Entwicklungsprojekt, grant no. DIK0249.

## REFERENCES

- [1] R. Bommasani, D. A. Hudson, E. Adeli, R. Altman, S. Arora, S. von Arx, M. S. Bernstein, J. Bohg, A. Bosselut, E. Brunskill *et al.*, “On the opportunities and risks of foundation models,” *arXiv preprint arXiv:2108.07258*, 2021.
- [2] C. Zhou, Q. Li, C. Li, J. Yu, Y. Liu, G. Wang, K. Zhang, C. Ji, Q. Yan, L. He *et al.*, “A comprehensive survey on pretrained foundation models: A history from bert to chatgpt,” *International Journal of Machine Learning and Cybernetics*, pp. 1–65, 2024.
- [3] R. Firoozi, J. Tucker, S. Tian, A. Majumdar, J. Sun, W. Liu, Y. Zhu, S. Song, A. Kapoor, K. Hausman *et al.*, “Foundation models in robotics: Applications, challenges, and the future,” *The International Journal of Robotics Research*, p. 02783649241281508, 2023.
- [4] C. Chi, Z. Xu, C. Pan, E. Cousineau, B. Burchfiel, S. Feng, R. Tedrake, and S. Song, “Universal manipulation interface: In-the-wild robot teaching without in-the-wild robots,” *arXiv preprint arXiv:2402.10329*, 2024.
- [5] Z. Fu, T. Z. Zhao, and C. Finn, “Mobile aloha: Learning bimanual mobile manipulation with low-cost whole-body teleoperation,” *arXiv preprint arXiv:2401.02117*, 2024.
- [6] T. Z. Zhao, J. Tompson, D. Driess, P. Florence, K. Ghasemipour, C. Finn, and A. Wahid, “Aloha unleashed: A simple recipe for robot dexterity,” *arXiv preprint arXiv:2410.13126*, 2024.
- [7] P. Wu, Y. Shentu, Z. Yi, X. Lin, and P. Abbeel, “Gello: A general, low-cost, and intuitive teleoperation framework for robot manipulators,” 2024. [Online]. Available: <https://arxiv.org/abs/2309.13037>
- [8] T. Inoue, G. De Magistris, A. Munawar, T. Yokoya, and R. Tachibana, “Deep reinforcement learning for high precision assembly tasks,” in *2017 IEEE/RSJ International Conference on Intelligent Robots and Systems (IROS)*. IEEE, 2017, pp. 819–825.
- [9] L. Johannsmeier, M. Gerchow, and S. Haddadin, “A framework for robot manipulation: Skill formalism, meta learning and adaptive control,” in *2019 International Conference on Robotics and Automation (ICRA)*. IEEE, 2019, pp. 5844–5850.
- [10] Y. Wu, F. Wu, L. Chen, K. Chen, S. Schneider, L. Johannsmeier, Z. Bing, F. J. Abu-Dakka, A. Knoll, and S. Haddadin, “1 khz behavior tree for self-adaptable tactile insertion,” in *2024 IEEE International Conference on Robotics and Automation (ICRA)*. IEEE, 2024, pp. 16 002–16 008.
- [11] Y. Wu, Z. Chen, F. Wu, L. Chen, L. Zhang, Z. Bing, A. Swikir, A. Knoll, and S. Haddadin, “Tacdiffusion: Force-domain diffusion policy for precise tactile manipulation,” *arXiv preprint arXiv:2409.11047*, 2024.
- [12] A. Brohan, N. Brown, J. Carbajal, Y. Chebotar, J. Dabis, C. Finn, K. Gopalakrishnan, K. Hausman, A. Herzog, J. Hsu *et al.*, “Rt-1: Robotics transformer for real-world control at scale,” *arXiv preprint arXiv:2212.06817*, 2022.
- [13] P. Sharma, L. Mohan, L. Pinto, and A. Gupta, “Multiple interactions made easy (mime): Large scale demonstrations data for imitation,” in *Conference on robot learning*. PMLR, 2018, pp. 906–915.
- [14] E. Jang, A. Irpan, M. Khansari, D. Kappler, F. Ebert, C. Lynch, S. Levine, and C. Finn, “Bc-z: Zero-shot task generalization with robotic imitation learning,” in *Conference on Robot Learning*. PMLR, 2022, pp. 991–1002.
- [15] H.-S. Fang, H. Fang, Z. Tang, J. Liu, J. Wang, H. Zhu, and C. Lu, “Rh20t: A robotic dataset for learning diverse skills in one-shot,” in *RSS 2023 Workshop on Learning for Task and Motion Planning*, 2023.

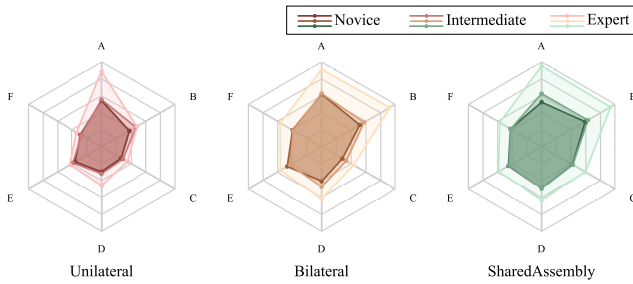


Fig. 6: Task Efficiency across methods and participants with different background.

Participants exhibit a significantly higher success rate across all teleoperation modes. Besides, prior experience with robot usage also contributes to participants’ overall success rate, though its effect is less pronounced than that of teleoperation experience. The results indicate that long-term practice contributes to the improvement of users’ tele-assembly task success rate. It is worth mentioning that intermediate operators using our SharedAssembly even surpass teleoperation experts using Bilateral teleoperation, resulting in a 97.2% success rate. In addition, novice and intermediate users with our method achieve performance comparable to experts using baseline methods. As a result, our method can significantly lower the operator’s skill barrier and corresponding training period.

Following the Common Industry Format for Usability Test Reports (ISO/IEC 25062:2006) [36], we use the efficiency as the performance metric to measure the method’s data collection efficiency, defined as the ratio of the task completion rate to the mean time per task (measured in minutes). As depicted in Fig. 6, *SharedAssembly* demonstrates top-tier performance across diverse user groups and task scenarios, exhibiting both high efficiency and generalizability.

These results showcase that our data collection approach significantly enhances efficiency in tight-clearance tele-assembly tasks while reducing the training cycle for data collectors. Therefore, it holds strong potential in facilitating rapid and large-scale data collection, paving the way for further research towards general-purpose intelligent robots.

## VII. CONCLUSION

In this work, we present a novel *Bilateral* Teleoperation approach for contact-rich assembly tasks. By incorporating prior knowledge of tight-clearance assembly through *SharedAssembly*, our approach significantly improves the execution speed and success rate compared to comparing baselines, achieving a 97.0% success rate across various *sub-millimeter-level* assembly tasks. Extensive experiments validate the effectiveness of our approach in real-world data collection, demonstrating its potential for scalable acquisition of contact-rich robotic manipulation data. For future work, we aim to extend our method to long-horizon manipulation tasks and integrate more perception techniques to further assist operators in teleoperation. Additionally, we aim to train the foundation model using the collected dataset to improve the performance in assembly tasks.

- [16] H. Bharadhwaj, J. Vakil, M. Sharma, A. Gupta, S. Tulsiani, and V. Kumar, "Roboagent: Generalization and efficiency in robot manipulation via semantic augmentations and action chunking," in *2024 IEEE International Conference on Robotics and Automation (ICRA)*. IEEE, 2024, pp. 4788–4795.
- [17] H. R. Walke, K. Black, T. Z. Zhao, Q. Vuong, C. Zheng, P. Hansen-Estruch, A. W. He, V. Myers, M. J. Kim, M. Du *et al.*, "Bridgedata v2: A dataset for robot learning at scale," in *Conference on Robot Learning*. PMLR, 2023, pp. 1723–1736.
- [18] A. Khazatsky, K. Pertsch, S. Nair, A. Balakrishna, S. Dasari, S. Karamcheti, S. Nasiriany, M. K. Srirama, L. Y. Chen, K. Ellis *et al.*, "Droid: A large-scale in-the-wild robot manipulation dataset," in *Robotics: Science and Systems*, 2024.
- [19] A. O'Neill, A. Rehman, A. Maddukuri, A. Gupta *et al.*, "Open x-embodiment: Robotic learning datasets and rt-x models: Open x-embodiment collaboration 0," in *2024 IEEE International Conference on Robotics and Automation (ICRA)*. IEEE, 2024, pp. 6892–6903.
- [20] K. Wu, C. Hou, J. Liu, Z. Che, X. Ju, Z. Yang, M. Li, Y. Zhao, Z. Xu, G. Yang *et al.*, "Robomind: Benchmark on multi-embodiment intelligence normative data for robot manipulation," *arXiv preprint arXiv:2412.13877*, 2024.
- [21] D. Sliwowski, S. Jadav, S. Stanovic, J. Orbik, J. Heidersberger, and D. Lee, "Reassemble: A multimodal dataset for contact-rich robotic assembly and disassembly," *arXiv preprint arXiv:2502.05086*, 2025.
- [22] J. Aldaco, T. Armstrong, R. Baruch, J. Bingham, S. Chan, K. Draper, D. Dwibedi, C. Finn, P. Florence, S. Goodrich *et al.*, "Aloha 2: An enhanced low-cost hardware for bimanual teleoperation," *arXiv preprint arXiv:2405.02292*, 2024.
- [23] V. Nitsch and B. Färber, "A meta-analysis of the effects of haptic interfaces on task performance with teleoperation systems," *IEEE transactions on haptics*, vol. 6, no. 4, pp. 387–398, 2012.
- [24] S. Sujit, L. Nunziant, D. O. Lillrank, R. F. J. Dossa, and K. Arulkumar, "Improving low-cost teleoperation: Augmenting gello with force," in *2025 IEEE/SICE International Symposium on System Integration (SII)*. IEEE, 2025, pp. 747–752.
- [25] A. Pervez, A. Ali, J.-H. Ryu, and D. Lee, "Novel learning from demonstration approach for repetitive teleoperation tasks," in *2017 IEEE World Haptics Conference (WHC)*. IEEE, 2017, pp. 60–65.
- [26] X. Chen, T. Ni, K. Karacan, H. Sadeghian, and S. Haddadin, "Online transfer and adaptation of tactile skill: A teleoperation framework," in *8th Annual Conference on Robot Learning*, 2024. [Online]. Available: <https://openreview.net/forum?id=6X3ybeVpDi>
- [27] M. Selvaggio, M. Cagnetti, S. Nikolaidis, S. Ivaldi, and B. Siciliano, "Autonomy in physical human-robot interaction: A brief survey," *IEEE Robotics and Automation Letters*, vol. 6, no. 4, pp. 7989–7996, 2021.
- [28] M. M. Marinho, H. Ishida, K. Harada, K. Deie, and M. Mitsuishi, "Virtual fixture assistance for suturing in robot-aided pediatric endoscopic surgery," *IEEE Robotics and Automation Letters*, vol. 5, pp. 524–531, 2019.
- [29] M. Laghi, M. Maimeri, M. Marchand, C. Leparoux, M. Catalano, A. Ajoudani, and A. Bicchi, "Shared-autonomy control for intuitive bimanual tele-manipulation," in *2018 IEEE-RAS 18th International Conference on Humanoid Robots (Humanoids)*. IEEE, 2018, pp. 1–9.
- [30] G. Quere, A. Hagengruber, M. Iskandar, S. Bustamante, D. Leidner, F. Stulp, and J. Vogel, "Shared control templates for assistive robotics," in *2020 IEEE international conference on robotics and automation (ICRA)*. IEEE, 2020, pp. 1956–1962.
- [31] X. Chen, Y. Michel, H. Sadeghian, and S. Haddadin, "Network-aware shared autonomy in bilateral teleoperation," in *2024 IEEE-RAS 23rd International Conference on Humanoid Robots (Humanoids)*. IEEE, 2024, pp. 888–894.
- [32] X. Chen, H. Sadeghian, L. Chen, M. Tröbinger, A. Swirkir, A. Naciri, and S. Haddadin, "A passivity-based approach on relocating high-frequency robot controller to the edge cloud," in *2023 IEEE International Conference on Robotics and Automation (ICRA)*. IEEE, 2023, pp. 5242–5248.
- [33] A. K. Gupta and V. Govindarajan, "Knowledge flows and the structure of control within multinational corporations," *Academy of management review*, vol. 16, no. 4, pp. 768–792, 1991.
- [34] M. Calabrese, A. Amato, V. D. Lecce, and V. Piuri, "Hierarchical-granularity holonic modelling," *Journal of Ambient Intelligence and Humanized Computing*, vol. 1, pp. 199–209, 2010.
- [35] E. Burdet, D. W. Franklin, and T. E. Milner, *Human robotics: neuromechanics and motor control*. MIT press, 2013.
- [36] B. Albert and T. Tullis, *Measuring the user experience: collecting, analyzing, and presenting usability metrics*. Newnes, 2013.